Amine−Hydrogen Halide Complexes: Experimental Electric Dipole Moments and a Theoretical Decomposition of Dipole Moments and Binding Energies

Carolyn S. Brauer,[†] Matthew B. Craddock,[‡] Jacob Kilian,[†,§] Erik M. Grumstrup,[†] M. Christopher Orilall,[||] Yirong Mo,[⊥] Jiali Gao,*[,†,§] and Kenneth R. Leopold*[,†]

Department of Chemistry, University of Minnesota, 207 Pleasant Street, SE, Minneapolis, Minnesota 55455, Supercomputing Institute, University of Minnesota, Minneapolis, Minnesota 55455, and Department of Chemistry, Western Michigan University, Kalamazoo, Michigan 49008

Received: April 4, 2006; In Final Form: June 26, 2006

The Stark effect has been observed in the rotational spectra of several gas-phase amine−hydrogen halide complexes and the following electric dipole moments have been determined: $H_3{}^{15}N-H^{35}Cl$ (4.05865 ± 0.00095 D), $(CH_3)_3{}^{15}N-H^{35}Cl$ (7.128 ± 0.012 D), $H_3{}^{15}N-H^{79}Br$ (4.2577 ± 0.0022 D), and $(CH_3)_3{}^{15}N-H^{79}Br$ (8.397 ± 0.014 D). Calculations of the binding energies and electric dipole moments for the full set of complexes $R_n(CH_3)_{3-n}N-HX$ ($n = 0-3$; X = F, Cl, Br) at the MP2/aug-cc-pVDZ level are also reported. The block localized wave function (BLW) energy decomposition method has been used to partition the binding energies into contributions from electrostatic, exchange, distortion, polarization, and charge-transfer terms. Similarly, the calculated dipole moments have been decomposed into distortion, polarization, and charge-transfer components. The complexes studied range from hydrogen-bonded systems to proton-transferred ion pairs, and the total interaction energies vary from 7 to 17 kcal/mol across the series. The individual energy components show a much wider variation than this, but cancellation of terms accounts for the relatively narrow range of net binding energies. For both the hydrogen-bonded complexes and the proton-transferred ion pairs, the electrostatic and exchange terms have magnitudes that increase with the degree of proton transfer but are of opposite sign, leaving most of the net stabilization to arise from polarization and charge transfer. In all of the systems studied, the polarization terms contribute the most to the induced dipole moment, followed by smaller but still significant contributions from charge transfer. A significant contribution to the induced moment of the ion pairs also arises from distortion of the HX monomer.

Introduction

Complexes formed from amines and hydrogen halides are simple prototypes in which to study hydrogen bonding and proton transfer.[1−11] First observed in Knudsen cell studies,[1] and later investigated in a classic series of matrix isolation experiments,[2,3] these systems have attracted the attention of researchers for decades. A key issue which permeates their study concerns the possibility of an acid−base reaction within the complex, and indeed much of the work on these systems has been aimed at both assessing the degree of proton transfer and understanding the factors which influence it. Recent years have seen a revival of activity in this area, particularly in the form of matrix infrared studies,[4] which have explored the effects of amine basicity, the identity of the halide, and the composition of the host medium on proton transfer across the hydrogen bond. Collectively, this work has shown that the nature of the acid and base, as well as the polarizability of the surroundings, combine to give a wide range of binding types in low-temperature matrixes. Thus, for example, H_3N-HF in an argon host is a strongly hydrogen-bonded complex,[3b] but $(CH_3)_3N-HBr$ in an N_2 host is best described as a $(CH_3)_3NH^+Br^-$ ion pair.[3f]

Gas-phase studies have also investigated the extent of proton transfer in these systems.[5,6] Legon, in particular,[5] has reported a series of microwave spectroscopic studies on complexes of H_3N, $(CH_3)H_2N$, and $(CH_3)_3N$ with the full set of hydrogen halides and has used force constants and nuclear quadrupole coupling constants to estimate the degree of proton transfer in the isolated adducts. The results have demonstrated that the isolated 1:1 gas-phase complexes H_3N-HX are hydrogen-bonded, with little or no sign of ion pair formation. However, as in low-temperature matrixes, increased methylation of the ammonia, together with use of the heavier, more acidic hydrogen halides stabilizes the ion-pair form. Thus, H_3N-HF is a hydrogen-bonded system, but the complex formed from $(CH_3)_3N$ and HI is best regarded as a $(CH_3)_3NH^+I^-$ ion pair, even in the gas phase. The effect of an additional HF molecule on proton transfer in H_3N-HF has also been investigated both experimentally[3g,6] and theoretically.[6,8e,g]

The application of computational methods to these systems has also been vigorously pursued.[7−9] Indeed, published studies have detailed the structures and binding energies of a wide variety of amine−HX complexes and have explored their potential energy surfaces along the proton-transfer coordinate.[7] Small clusters containing several NH_3 and hydrogen halide units have been investigated for the purpose of characterizing the influence of near-neighbor interactions on the transition from hydrogen bonding to ion pairs,[6,8b,e,g,f,9] and calculations on H_3N-HX complexes with several water molecules have been per-

[†] Department of Chemistry, University of Minnesota.
[‡] Present address: Department of Chemistry, Columbia University, New York, NY 10027.
[§] Supercomputing Institute, University of Minnesota.
[||] Present address: Department of Chemistry, Cornell University, Ithaca, NY 14853-1301.
[⊥] Western Michigan University.

10.1021/jp062101a CCC: $33.50
Published on Web 07/29/2006

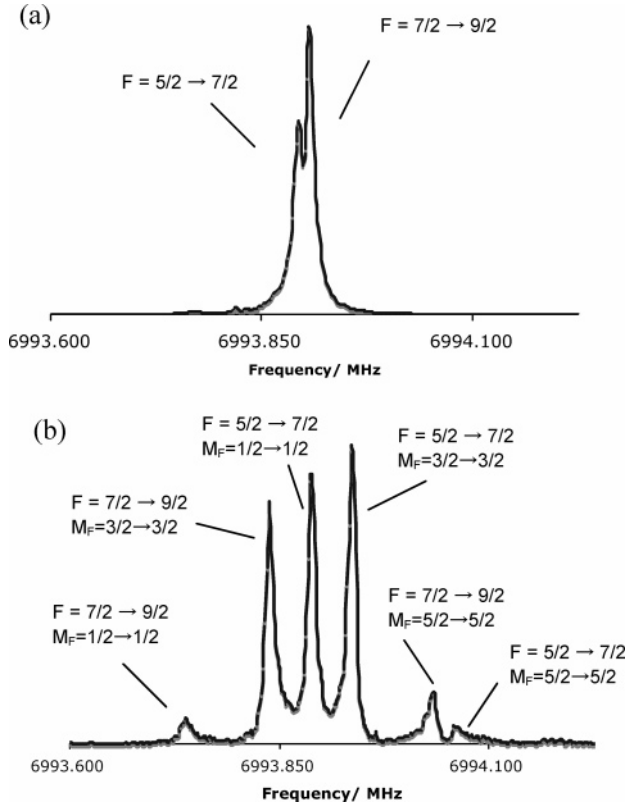

Figure 1. $F = {}^{7}/_{2} \leftarrow {}^{5}/_{2}$ and $F = {}^{9}/_{2} \leftarrow {}^{7}/_{2}$ components in the $J = 3 \leftarrow 2$, $K = 0$ transition of $(CH_3)_3{}^{15}N-H^{79}Br$: (a) field-free; (b) at an electric field strength of 37.7 V/cm. These are $\Delta M_F = 0$ lines, in which the electric field vector of the microwave radiation is oriented parallel to the direction of the static electric field.

formed with a similar goal.[9b,c] Calculation of matrix shifts in the infrared spectra have also been carefully explored, providing a direct complement to experimental matrix isolation work.[10]

Despite the simplicity and general appeal of amine−HX complexes, one feature that has not received wide attention is the electric dipole moment. Although several papers have reported theoretical values for a number of the R_3N-HX systems,[8b,i,j,9b−d] it appears that none of the dipole moments for these complexes have been determined experimentally. Moreover, although theoretical values of the electric dipole moments may be readily obtained, the physical origins of the polarity in these systems have not been thoroughly elucidated, at least to the extent now possible by modern computational methods. The dipole moment is a simple, fundamental measure of charge distribution and should therefore be intrinsically relevant to the degree of proton transfer. Moreover, experimental dipole moments offer a useful reference point for calculations concerned with the interactions between R_3N-HX complexes and matrix environments. In this paper, therefore, we report the experimental determination of the gas-phase electric dipole moments of four amine−hydrogen halide complexes: R_3N-HX ($R = H, CH_3$; $X = Cl, Br$). The results are then complemented with an extensive set of calculations on a larger series of amine−HX systems using the Block Localized Wave function (BLW) energy decomposition method,[11−13] in which both the dipole moments and binding energies are broken down into physically meaningful contributions from electrostatic, polarization, distortion, and charge-transfer terms. Thus, the combined results of theory and experiment provide a particularly complete and accurate picture of the degree and sources of polarity and binding in these prototypical systems, and should serve as valuable benchmarks for the study of hydrogen bonding and proton transfer.

TABLE 1: Zero-Field Spectroscopic Constants for $(CH_3)_3{}^{15}N-H^{79}Br$

	$(CH_3)_3{}^{15}N\cdots H^{79}Br$
B (MHz)	1165.88725(48)
D_J (kHz)	0.131(18)
D_{JK} (kHz)	7.742(86)
eQq(^{79}Br) (MHz)	119.1966(63)

Experimental Methods and Results

Stark−shifted rotational spectra were recorded using a pulsed nozzle Fourier transform microwave spectrometer[14] and used to obtain experimental values for molecular electric dipole moments. Details of the spectrometer have been given elsewhere.[15] Briefly, the system is equipped with a pair of removable, rectangular aluminum Stark plates, which operate in a bipolar configuration and straddle the microwave cavity to apply a uniform dc electric field perpendicular to both the cavity axis and the direction of the supersonic jet.[16,17] For the systems studied in this work, several transitions previously assigned at zero electric field were examined at a series of field strengths. Little, if any, spectral broadening occurred as the electric field strength was increased, but the intensity of the transitions was observed to diminish. In most cases, this ultimately limited the degree to which transitions could be shifted, but the problem was not severe enough to preclude sufficiently accurate determination of the dipole moments. Because the orientation of the microwave antenna relative to the direction of the electric field can be adjusted, both $\Delta M_F = 0$ and $\Delta M_F = \pm 1$ were readily observed in this work.

The effective plate spacing for each experiment (needed to calculate the electric field strengths from measurements of the applied voltage) was determined by calibration using the $J = 1 \leftarrow 0$ transition of OCS ($\mu = 0.715\,21(20)$ D).[18] To eliminate possible errors due to the accumulation of diffusion pump oil on the plate surfaces,[16,19] calibrated distances were obtained both before and after the collection of experimental data, and the data were admitted for analysis only upon agreement of the pre- and postcollection values. For this reason, experiments were found to be best performed during the winter months when cooling water for the diffusion pump was colder and backstreaming, therefore, reduced.

The molecular source used to prepare the jet-cooled complexes consisted of a General Valve Series 9 pulsed nozzle for which a small piece of stainless steel hypodermic tubing (0.016 in. i.d.) was fitted so as to introduce a continuously flowed gas into the central portion of the supersonic expansion. The general design is similar to that used by other groups,[20] and identical to that used previously in our laboratory.[21] For the HCl complexes, a mixture of 0.5% NH_3 or $(CH_3)_3N$ in Ar at a stagnation pressure of 15 psig was pulsed through a 0.8 mm diameter orifice at a repetition rate of 5 Hz. A flow of neat HCl, metered by a mass flow controller (MKS Corporation), entered the expansion through the hypodermic needle at a rate of 5 standard cubic centimeters per minute (sccm). For H_3N-HBr, a 0.5% mixture of NH_3 in Ar was expanded at a stagnation pressure of approximately 35−40 psig and an HBr flow rate of 35 sccm was used. For experiments on $(CH_3)_3N-HBr$, a 0.25% mixture expanded at a stagnation pressure of 27 psig, but with a lower HBr flow rate of 5 sccm. A sample spectrum, showing a portion of the $J = 3 \leftarrow 2$, $K = 0$ transition of $(CH_3)_3{}^{15}N-H^{79}Br$ taken at (a) 0.0 V/cm and (b) 37.7 V/cm, is shown in

TABLE 2: Summary of Stark Effect Measurements

molecule	transitions examined	F′ ← F″	range of electric fields strengths (V/cm)	N^a	μ (Debye)^b	$\Delta\mu_{ind}$ (Debye)^c
$H_3{}^{15}N-H^{35}Cl$	$J = 1 \leftarrow 0, K = 0$	0.5 ← 1.5	0.6−161.8	68	4.05865(95)	1.4787(16)
		1.5 ← 1.5				
		2.5 ← 1.5				
	$J = 2 \leftarrow 1, K = \pm 1$	1.5 ← 1.5				
$(CH_3)_3{}^{15}N-H^{35}Cl$	$J = 2 \leftarrow 1, K = 0$	1.5 ← 1.5	12.4−62.1	74	7.128(12)	5.408(16)
		2.5 ← 1.5				
		3.5 ← 2.5				
$H_3{}^{15}N-H^{79}Br$	$J = 1 \leftarrow 0, K = 0$	0.5 ← 1.5	15.4−80.0	69	4.2577(22)	1.9591(27)
		2.5 ← 1.5				
$(CH_3)_3{}^{15}N-H^{79}Br$	$J = 3 \leftarrow 2, K = 0$	3.5 ← 2.5	12.6−88.1	109	8.397(14)	6.958(17)
		4.5 ← 3.5				

[a] Total number of transitions in fit. Includes measured zero-field frequencies. [b] Numbers in parentheses are one standard error in the least-squares fit. [c] $\Delta\mu_{ind} = \mu(\text{complex}) - \mu(\text{HX}) - \mu(R_3N)$.

Figure 1. Complete listings of spectral frequencies and electric field strengths for all complexes studied are available as Supporting Information.

To eliminate the complicating effects of ^{14}N nuclear quadrupole coupling, all spectra were recorded for the ^{15}N isotopically substituted species. $^{15}NH_3$ was synthesized as described previously[22] from the reaction of solid KOH with solid $^{15}NH_4Cl$ (Icon Isotopes, 99.5 atom percent), which gave essentially quantitative yield. $(CH_3)_3{}^{15}N$ was prepared according to literature procedures[23] by first heating $^{15}NH_4Cl$ and paraformaldehyde (Aldrich) to form $(CH_3)_3{}^{15}NH^+Cl^-$. Free $(CH_3)_3{}^{15}N$ was then released by addition of concentrated NaOH solution and collected in a small evacuated ballast.

The observed transitions for $H_3{}^{15}N-HCl$,[24] $(CH_3)_3{}^{15}N-HCl$,[25] and $H_3{}^{15}N-HBr$[26] were readily located at zero electric field on the basis of published work. For $(CH_3)_3{}^{15}N-HBr$, however, previously reported spectra[27] did not include observations of the ^{15}N substituted form, and for this reason a total of 37 field-free lines (covering three rotational transitions) of $(CH_3)_3{}^{15}N-H^{79}Br$ were recorded prior to observation of the Stark effect. The observed transition frequencies, provided as Supporting Information, were fitted to the usual Hamiltonian for a symmetric rotor with one quadrupolar nucleus,[28] and the resulting spectroscopic constants are given in Table 1.

Stark-shifted spectra were analyzed using the program QSTARK,[29,30] which performs a complete diagonalization of the full rotational energy matrix:

$$\mathbf{H} = \mathbf{H}_{rot.} + \mathbf{H}_{quad} + \mathbf{H}_{Stark} \quad (1)$$

Here $\mathbf{H}_{rot.}$ is the semirigid rotor rotational Hamiltonian, including centrifugal distortion, $\mathbf{H}_{quad}$ accounts for nuclear quadrupole coupling, and $\mathbf{H}_{Stark} = -\boldsymbol{\mu}\cdot\mathbf{E}$ (where $\mathbf{E}$ is the electric field strength and $\boldsymbol{\mu}$ is the molecular electric dipole moment). The Hamiltonian matrix is constructed in the $|I,J,F,M_F\rangle$ basis using matrix elements reported previously.[31−33] The dipole moment of each complex was obtained from a least-squares fit of the observed Stark-shifted frequencies with the rotational and (^{79}Br) nuclear quadrupole coupling constants constrained to their previously determined zero-field values. Examination of the observed Stark shifts indicated that for $^{15}NH_3-H^{79}Br$, the Stark effects were essentially second order, whereas for $(CH_3)_3{}^{15}N-H^{79}Br$, $H_3{}^{15}N-H^{35}Cl$ and $(CH_3)_3{}^{15}N-H^{35}Cl$, significant deviations were observed for some components, requiring the full diagonalization performed by QSTARK.[34] The resulting dipole moments are given in Table 2, together with a summary of the number and identity of transitions analyzed, and the range of electric field strengths used. Values of the induced dipole moments, defined by $\Delta\mu_{ind} \equiv \mu(\text{complex}) - \mu(\text{HX}) - \mu(R_3N)$, are also listed in the table. In obtaining these values, the experimental electric dipole moments of HCl (1.1085 ± 0.0005 D),[35] $H^{79}Br$ (0.8271 ± 0.0003 D),[36] $^{14}NH_3$ (1.47149 ± 0.00015 D),[37] and $(CH_3)_3N$ (0.612 ± 0.003 D)[38] were used.

Computational Methods and Results

Calculations were performed for a series of amine−HX complexes using the BLW program[39] and the Gaussian 03 package of computer codes.[40] Binding energies, defined as the difference in energies between the complex at its MP2 optimum geometry and the free monomers at their optimum geometries, were computed at the Hartree−Fock level of theory and corrected for basis set superposition error using the counterpoise correction of Boys and Bernardi,[41] viz.

$$\Delta E_{HF} = E_{HF}[\psi(DA)] - E_{HF}{}^{o}[\psi^{o}(D^{o})] - E_{HF}{}^{o}[\psi^{o}(A^{o})] + \Delta E_{BSSE} \quad (2)$$

where D and A represent the donor and acceptor, respectively, and the superscript "o" refers to the isolated monomer at its equilibrium geometry. For post Hartree−Fock calculations, the interaction energy, ΔE_{int}, is defined as the sum of the Hartree−Fock interaction energy and a correction component due to electron correlation, approximated here by Møller−Plesset second-order perturbation theory (MP2, with core orbitals frozen), i.e.

$$\Delta E_{int} = \Delta E_{HF} + \Delta\Delta E_{MP2} \quad (3)$$

In the calculation of ΔE_{int}, the counterpoise correction was performed at the MP2 level.

Electric dipole moments were also calculated for both the monomers and the adduct. A number of basis sets were tested, including 6-31G(d), aug-cc-pVDZ, 6-31+G(d,p), and 6-311++G(d,p), for both energy and dipole moment calculations, but for the most part, only those corresponding to the aug-cc-pVDZ calculations are reported here. These tests demonstrated good convergence with respect to basis set, and the results and trends are generally consistent among basis sets, except as noted in the discussion which follows. Detailed comparisons between basis sets can be found elsewhere.[42]

TABLE 3: Comparison between Observed and Calculated Properties[a] for Amine−HX Complexes and Their Constituent Monomers

complex	exptl bond length[b]	calcd bond length[c]	% diff	μ exptl	μ calcd[c]	% diff
		R(N···X)				
H_3N-HCl	3.1358(7)[d]	3.068	−2.2	4.05865(95)	4.78	17.8
H_3N-HBr	3.2540[e]	3.193	−1.9	4.2577(22)	4.92	15.6
$(CH_3)_3N-HCl$	2.8166(3)[f]	2.822	0.2	7.128(12)	8.72	22.3
$(CH_3)_3N-HBr$	2.9594[b,g]	2.983	0.8	8.397(14)	9.77	16.4
		r_e(HX) or r_e(HN)				
HF	0.9169[h,i]	0.925	−0.9	1.826178(3)[j]	1.95	6.8
HCl	1.2746[i]	1.288	0.0	1.1085(5)[k]	1.26	13.7
HBr	1.4145[i]	1.420	−0.4	0.8271(3)[l]	0.99	19.7
NH_3	1.0114[h]	1.020	−0.9	1.47149(15)[m]	1.64	11.5

[a] All distances are in angstroms. All dipole moments are in Debye. [b] Values correspond to ^{15}N complexes, except for $(CH_3)_3N-HBr$, for which the ^{14}N value was used. [c] Calculated at the HF/aug-cc-pVDZ level/basis set. [d] Reference 24. [e] Reference 26. [f] Reference 25. [g] Ion pair value of ref 27. [h] Reference 43. [i] Reference 44. [j] $J = 1$ value of ref 46. [k] $J = 1$ value of ref 35. [l] Reference 36. [m] $J = 1$, $K = 0$ value of ref 37.

TABLE 4: Selected Bond Lengths for Amine−HX Complexes Calculated at the MP2/aug-cc-pVDZ Level[a]

complex	r(N−X)	r(H−X)	r(N···H)	Δr(H−X)	ρ_{PT}[b]
H_3N-HF	2.647	0.960	1.687	0.035	−0.632 (−0.661)
$(CH_3)H_2N-HF$	2.605	0.969	1.638	0.044	−0.574 (−0.608)
$(CH_3)_2HN-HF$	2.574	0.978	1.599	0.053	−0.526 (−0.568)
$(CH_3)_3N-HF$	2.555	0.984	1.571	0.059	−0.492 (−0.541)
H_3N-HCl	3.068	1.343	1.725	0.055	−0.650 (−0.773)
$(CH_3)H_2N-HCl$	2.914	1.405	1.514	0.117	−0.377 (−0.603)
$(CH_3)_2HN-HCl$	2.814	1.637	1.185	0.349	+0.184 (−0.309)
$(CH_3)_3N-HCl$	2.822	1.656	1.167	0.221	+0.221 (+0.139)
H_3N-HBr	3.193	1.487	1.706	0.066	−0.619 (−0.749)
$(CH_3)H_2N-HBr$	2.967	1.812	1.164	0.391	+0.248 (+0.216)
$(CH_3)_2HN-HBr$	2.974	1.856	1.133	0.436	+0.323 (+0.304)
$(CH_3)_3N-HBr$	2.983	1.856	1.127	0.435	+0.329 (+0.326)

[a] Energies are in kcal/mol. Bond lengths are in angstroms. [b] Value in parentheses is determined at the MP2/6-311++G(d,p) level of theory.

Although the total energies were calculated at both the Hartree−Fock and MP2 levels, the dipole moment calculations and the BLW decompositions (described below) were done at the Hartree−Fock level only.

Table 3 contains observed and calculated bond lengths and electric dipole moments of complexes for which experimental data are available. Also included are equilibrium bond lengths and dipole moments for HF, HCl, HBr, and NH_3. Table 4 provides selected bond lengths for a wider range of complexes, including many for which experimental data are not available. For the complexes, it is seen from Table 3 that at the MP2/aug-cc-pVDZ level of theory, bond lengths are generally accurate to within about 2%, whereas the dipole moments at the HF/aug-cc-pVDZ level agree with experiment to within about 20%. It should be noted that the experimental results are vibrationally averaged, and the theoretical values are not. Moreover, the experimental bond lengths are derived by assuming invariant monomer geometries upon complexation. Nonetheless, the 2% agreement for the intermolecular bond lengths is satisfying and fairly typical. The comparisons between experimental and theoretical dipole moments, on the other hand, may be more susceptible to vibrational averaging effects. The HF/aug-cc-pVDZ calculations appear to systematically overestimate the electric dipole moments, and angular vibrational motion of the amine and HX moieties can contribute, in part, to the difference. For example, for H_3N-HCl, using Legon's excursion angles of 21.7° and 23° for the H_3N and HCl, respectively,[24] together with the experimental dipole moments of the monomers, gives a projective reduction in the dipole moment of the complex of 0.19 D. Thus, angular vibrational averaging accounts for a small, but not insignificant, fraction of the 0.72 D discrepancy between experimental and calculated values. Similar estimates for the other complexes can be made using approximate excursion angles given in refs 24−27. The results are smaller than those obtained for H_3N-HCl and do not likely account for a large part of the difference between theory and experiment.

Vibrational averaging along the umbrella coordinate of the amine moieties could also lower the observed value of the electric dipole moment. The calculated structures of the complexes do indicate a flattening of several degrees of the equilibrium structure of the amine upon complexation, and although it is not possible to say how much this changes the *vibrationally averaged* umbrella angle, a change of a few degrees is not unreasonable. Using the dipole moment surface of NH_3 calculated by Rosmus et al.,[47] we estimate a change in electric dipole moment of about 0.05 D/deg in the vicinity of the potential minimum (where the angle measured is that between the NH bond and the C_3 axis of the molecule). Thus, a change of several degrees could account for a reduction in electric dipole moment of several tenths of a Debye. Again, this is not enough to account for all of the discrepancy between theory and experiment, but it is not necessarily an insignificant contribution. The effect is expected to be smaller for complexes of $(CH_3)_3N$ complexes, given its smaller electric dipole moment and larger mass.

For most complexes, the calculations consistently yielded a single minimum in the potential energy surface. In the case of H_3N-HBr, however, calculations at the MP2/6-31+G(d,p) level produced two structures, a global minimum corresponding to an hydrogen-bonded form with a long N···HBr distance, and another proton-transferred form with structure and electric dipole moment resembling that of an $NH_4^+Br^-$ ion pair. This result is similar to that reported previously by Jordan and Del Bene.[10c] With an increase in the size of the basis set, however (i.e., at the MP2/aug-cc-PVDZ or MP2/6-311++G(d,p) levels), the ion

pair minimum vanished and only a single, hydrogen-bonded structure was determined. For this reason, only the hydrogen-bonded structure is discussed in this work.

As noted above, the BLW energy decomposition method of Mo et al.[11−13] was used to further investigate the details of complex formation in these systems. Though a number of approaches exist for this type of decomposition,[48−51] the definitions of individual energy terms vary among the methods. The BLW calculation gives the same electrostatic interaction energy as that of Morokuma[50] but differs in its calculation of the polarization and charge-transfer energies. Moreover, in comparison with the Morokuma approach, the BLW method is found to be less dependent on basis set.[11] Although the MP2 interaction energy consists of the HF interaction energy and electron correlation terms (eq 3), in the BLW calculation, only the HF interaction energy is decomposed, so the electron correlation and dispersion interactions beyond Hartree−Fock theory are not further partitioned. All BLW calculations were performed at the MP2 optimized optimum geometries.

Details of the BLW method have been given elsewhere[11−13] and only a brief summary and definition of terms is presented here. A main feature of the BLW approach is that a series of intermediate wave functions is constructed that specify well-defined charge densities, and the interaction is decomposed into a sum of geometric distortion (ΔE_{dist}), electrostatic (ΔE_{es}), exchange repulsion (ΔE_{ex}), polarization (ΔE_{pol}), and charge-transfer (ΔE_{ct}) terms:

$$\Delta E_{HF} = \Delta E_{dist} + \Delta E_{ex} + \Delta E_{pol} + \Delta E_{ct} \quad (4)$$

In this equation, ΔE_{dist} contains two terms, one for each monomer, and is defined as the energy difference between the monomers at their distorted configurations in the complex and at their free-molecule, equilibrium structures. In terms of the monomer wave functions, Ψ^o, ΔE_{dist} is given by

$$\Delta E_{dist} = \Delta E_{dist}(D) + \Delta E_{dist}(A) = E_{HF}[\Psi^o(D)] - E_{HF}[\Psi^o(D^o)] + E_{HF}[\Psi^o(A)] - E_{HF}[\Psi^o(A^o)] \quad (5)$$

where D and A refer to the HX donor and amine acceptor, respectively, in their distorted configurations in the complex and D^o and A^o refer to the isolated monomers. The electrostatic interaction energy is obtained by defining a reference state for the complex described by the nonantisymmetrized Hartree product, $\Phi_H^o(D,A) \equiv \Psi^o(D)\,\Psi^o(A)$ and computing

$$\Delta E_{es} = E[\Phi_H{}^o(D,A)] - E_{HF}[\Psi^o(D)] - E_{HF}[\Psi^o(A)] \quad (6)$$

The exchange energy follows from constructing the antisymmetrized wave function $\Phi^o(DA) \equiv \hat{A}\{\Phi_H^o(D,A)\}$ (where Φ is an antisymmetrization operator) and computing the resulting energy change:

$$\Delta E_{ex} = E[\Phi^o(DA)] - E[\Phi_H{}^o(D,A)] \quad (7)$$

The sum of ΔE_{es} and ΔE_{ex} is the total electrostatic interaction energy exclusive of polarization and is identical to the electrostatic interaction calculated by the method of Morokuma.

Although the molecular orbitals of each monomer are orthogonal, they are nonorthogonal between the two fragments, and when the exchange energy is calculated, an unoptimized, antisymmetric wave function, $\Phi^o(DA)$, is formed. This intermediate wave function can be variationally optimized with the restriction that the molecular orbitals on each monomer are not allowed to delocalize over the entire complex. In other words, each monomer's molecular orbitals are optimized in the presence of the other monomer. This optimization is achieved using the block-localized wave function (BLW) method, and the resulting block localized wave function is denoted $\Phi(DA) = \hat{A}\{\Psi(D)\,\Psi(A)\}$. Because this wave function allows charge reorganization within each monomer under the influence of the interacting partner, the energy change from the nonpolarized state gives the polarization energy:

$$\Delta E_{pol} = E[\Phi(DA)] - E[\Phi^o(DA)] \quad (8)$$

Finally, the restriction of the molecular orbital space to individual monomers is relaxed to include all basis function for the entire complex, which generates the Hartree−Fock Slater determinant wave function of the dimer DA. This process corresponds to charge delocalization from one molecular space to the other and provides the charge-transfer energy:

$$\Delta E_{ct} = E_{HF}[\Psi(DA)\,] - E[\Phi(DA)] + E_{BSSE} \quad (9)$$

The BSSE correction term is included in ΔE_{ct} because it is also concerned with the expansion of orbital basis similar to the change that occurs on going from $\Phi(DA)$ to $\Psi(DA)$. BSSE was computed at both HF and MP2 levels in the paper. The total interaction energy is at the MP2 level with BSSE(MP2) considered. The charge transfer was estimated at the HF level with the BSSE(HF) correction. The electron correlation is defined as an independent energy term in the BLW-ED method and dominated by the attractive dispersion effect, which is not considered in the HF method. Results of the energy decomposition for amine−HX complexes are presented in Table 5.

Application of the BLW method to the decomposition of molecular electric dipole moments has also been described.[13,17] Because of variations in monomer dipole moments across the series of systems studied, it is more convenient to analyze trends in the *induced* dipole moment than in the dipole moment itself. Contributions to the induced moment, calculated at the optimized geometries, are partitioned into those arising from distortion, polarization, and charge transfer, viz.

$$\Delta\mu_{ind}^{BLW} = \Delta\mu_{dist} + \Delta\mu_{pol} + \Delta\mu_{ct} \quad (10)$$

where $\Delta\mu_{dist}$ and $\Delta\mu_{pol}$ each represents the sum of two terms corresponding to each of the two monomers. $\Delta\mu_{dist}$ for either monomer is defined as the difference in electric dipole moment between a monomer in its distorted geometry in the complex, $\mu^o(X)$, and that of the free monomer, $\mu^o(X^o)$, calculated in the same basis set and level of theory. Thus

$$\Delta\mu_{dist} = [\mu^o(D) - \mu^o(D^o)] + [\mu^o(A) - \mu^o(A^o)] \quad (11)$$

$\Delta\mu_{pol}$ is calculated for each monomer using the individual component, $\Psi(D)$ or $\Psi(A)$, of the BLW wave function $\Phi(DA)$ and represents the change in polarity arising from the presence of the other monomer in the absence of charge transfer:

TABLE 5: Computed Interaction Energies and Energy Components from the Block Localized Wave Function Analysis, Calculated at HF/aug-cc-pVDZ Level with MP2/aug-cc-pVDZ Optimized Geometries[a]

	ΔE_{dist}								
complex	HX	R_3N	ΔE_{es}	ΔE_{ex}	ΔE_{es+ex}	ΔE_{pol}	ΔE_{ct}[b]	$\Delta\Delta E_{MP2}$	ΔE_{int}
H_3N-HF	2.1	0.0	−23.1	21.8	−1.3	−5.2	−5.0	−2.2	−11.6
$(CH_3)H_2N-HF$	2.8	0.1	−26.4	26.3	−0.1	−6.6	−6.0	−3.1	−12.9
$(CH_3)_2HN-HF$	3.6	0.1	−28.8	30.4	1.6	−8.0	−7.0	−3.8	−13.5
$(CH_3)_3N-HF$	4.2	0.1	−30.3	33.4	3.1	−9.3	−7.7	−4.2	−13.8
H_3N-HCl	1.5	0.0	−21.7	28.2	6.5	−6.2	−6.7	−3.5	−8.4
$(CH_3)H_2N-HCl$	5.3	0.1	−35.0	54.1	19.1	−14.7	−14.2	−5.9	−10.3
$(CH_3)_2HN-HCl$	29.5	1.0	−67.2	125.6	58.4	−58.1	−39.1	−4.4	−12.7
$(CH_3)_3N-HCl$	31.9	1.1	−70.3	131.1	60.8	−64.4	−40.5	−3.7	−14.8
H_3N-HBr	1.6	0.0	−22.7	33.3	10.6	−7.3	−8.1	−3.9	−7.1
$(CH_3)H_2N-HBr$	29.3	0.8	−70.7	142	71.3	−66.8	−43.1	−2.0	−10.5
$(CH_3)_2HN-HBr$	34.2	1.3	−77.7	153.3	75.6	−78.3	−45.9	−1.8	−14.9
$(CH_3)_3N-HBr$	34.1	1.5	−79.5	155.4	75.9	−81.5	−45.9	−1.4	−17.3

[a] All energies in kcal/mol. [b] Calculated using eq 9, which includes correction for BSSE.

$$\Delta\mu_{pol} = [\mu_{BLW}(D) - \mu^{o}(D)] + [\mu_{BLW}(A) - \mu^{o}(A)] \quad (12)$$

The charge-transfer component of the induced moment, $\Delta\mu_{ct}$, is the difference between the electric dipole moments of the complex obtained using the block localized wave function and the Hartree−Fock value, viz.

$$\Delta\mu_{ct}(DA) = \mu_{HF}(DA) - \mu_{BLW}(DA) \quad (13)$$

Calculated values of $\Delta\mu_{dist}$ and $\Delta\mu_{pol}$ at the HF/aug-cc-pVDZ level for the HX and amine components of the complexes studied, together with values of $\Delta\mu_{ct}$ and $\Delta\mu_{tot}$, are given in Table 6. Also included in the table are calculated values of $\Delta\mu_{ind}^{HF} \equiv \mu_{complex} - \mu_{HX} - \mu_{amine}$ obtained at the Hartree−Fock level of theory. In calculating the theoretical value of the induced dipole moment, the theoretical values of μ_{HX} and μ_{amine} were used. All results correspond to those obtained at the MP2/aug-cc-pDVZ optimized geometries.

Mulliken population analysis and Weinhold's natural population analysis[52,53] (NPA) were also employed to estimate atomic charges and thus the charge transfer between the two monomers. Although electric dipole moments were calculated with both the Hartree−Fock and BLW wave functions, partial atomic charges were calculated with Hartree−Fock theory only. The results are given in Table 7.

TABLE 6: Components of the Induced Electric Dipole Moments[a] for Amine−HX Complexes Arising from Distortion, Polarization, and Charge Transfer, Computed at the HF/aug-cc-pDVZ Level of Theory with MP2/aug-cc-pVDZ Optimized Geometries

	H−X		amine		dimer		
complex	$\Delta\mu_{dist}$	$\Delta\mu_{pol}$	$\Delta\mu_{dist}$	$\Delta\mu_{pol}$	$\Delta\mu_{ct}$	$\Delta\mu_{ind}^{BLW}$	$\Delta\mu_{ind}^{HF}$
H_3N-HF	0.07	0.39	−0.02	0.60	0.22	1.26	1.24
$(CH_3)H_2N-HF$	0.09	0.44	0.00	0.67	0.26	1.46	1.41
$(CH_3)_2HN-HF$	0.10	0.47	0.00	0.75	0.30	1.62	1.59
$(CH_3)_3N-HF$	0.12	0.49	0.00	0.88	0.33	1.82	1.79
H_3N-HCl	0.06	0.85	−0.03	0.53	0.45	1.86	1.89
$(CH_3)H_2N-HCl$	0.13	1.27	−0.05	0.82	0.74	2.91	2.98
$(CH_3)_2HN-HCl$	0.42	2.92	−0.09	1.67	0.91	5.83	6.13
$(CH_3)_3N-HCl$	0.44	3.09	−0.09	1.87	0.92	6.23	6.66
H_3N-HBr	0.04	1.10	−0.04	0.54	0.58	2.22	2.28
$(CH_3)H_2N-HBr$	0.27	3.73	−0.12	1.74	0.96	6.58	6.95
$(CH_3)_2HN-HBr$	0.31	4.15	−0.10	1.93	0.90	7.19	7.53
$(CH_3)_3N-HBr$	0.31	4.21	−0.11	2.08	0.93	7.42	7.97

[a] All values in Debye.

TABLE 7: Estimation of Charge Transfer to the HX Monomer Using Mulliken Population Analysis and Natural Population Analysis[a]

complex	Mulliken	NPA
H_3N-HF	0.049	−0.056
$(CH_3)H_2N-HF$	0.067	−0.068
$(CH_3)_2HN-HF$	0.231	−0.076
$(CH_3)_3N-HF$	0.37	−0.082
H_3N-HCl	0.094	−0.079
$(CH_3)H_2N-HCl$	0.077	−0.14
$(CH_3)_2HN-HCl$	−0.78	−0.71
$(CH_3)_3N-HCl$	−0.81	−0.72
H_3N-HBr	0.092	−0.091
$(CH_3)H_2N-HBr$	−0.67	−0.72
$(CH_3)_2HN-HBr$	−0.70	−0.74
$(CH_3)_3N-HBr$	−0.69	−0.74

[a] q(amine) = $-q$(HX).

Discussion

Structure and Bonding. As noted earlier, numerous workers have concluded, on the basis of both experimental and theoretical grounds, that H_3N-HX complexes are hydrogen-bonded, but that increasing methylation of the amine advances the degree of proton transfer. The experimental dipole moments presented in Table 2 are consistent with this notion. Because the transfer of a proton moves positive charge away from the negative halogen atom, progress toward ion pair formation is expected to increase the electric dipole moment of the complex. Indeed, we observe that the largest values of $\Delta\mu_{ind}$ occur for complexes of $(CH_3)_3N$, which are about 3.6 times greater than those of the corresponding complexes of NH_3, and approaching nearly 7 D for $(CH_3)_3N-HBr$. The increase in induced dipole moment on going from HCl to HBr for a given amine is somewhat more modest, about 30% between R_3N-HCl and R_3N-HBr. Nonetheless, all of the induced moments are large, and indicative of strong interactions.

Although the observed induced dipole moments increase as expected with amine basicity and HX acidity, the electric dipole moment is a complex quantity to which numerous factors contribute. Further insight into the nature of these complexes, therefore, is obtained by examining the theoretical results in Tables 4 and 5, which display structural and energetic aspects of complexes with varying degrees of methylation. The binding energies were calculated using eq 3, and included both basis set superposition error correction and electron correlation effects at the MP2 level. From a structural standpoint, the transition from hydrogen-bonded ("neutral") complexes to proton-transferred ion pairs is best inferred by the H−X and N···H distances. Specifically, for each of the hydrogen halides, increasing methylation of the amine is seen to render an

elongation of the H−X bond length and a corresponding decrease in the N···H bond distance. The simultaneous change in these distances, and their relationship to proton transfer, can be succinctly summarized by a single "proton-transfer parameter", ρ_{PT}, defined two decades ago by Kuring and Scheiner:[54]

$$\rho_{PT} = [r(H-X) - r^o(H-X)] - [r(N\cdots H) - r^o(N-H)] \quad (14)$$

Here, $r^o(H-X)$ and $r^o(N-H)$ are the HX and NH bond lengths in free HX and covalently bonded R_3NH^+, respectively, and $r(H-X)$ and $r(N\cdots H)$ are those in the complex of interest. Thus, ρ_{PT} assesses proton transfer according to how much the HX bond stretches in the complex *and* how much the N···H distance exceeds that in a system with full proton transfer. When $r(H-X) = r^o(H-X)$ and $r(N\cdots H) \gg r^o(N-H)$, the complex is best described as "hydrogen bonded" and $\rho_{PT} < 0$. On the other hand, when the proton has been transferred, the second term in eq 14 vanishes and $(H-X) \gg r^o(H-X)$, so that $\rho_{PT} > 0$. In the proton-shared regime, when the stretching of the HX bond is equal to the elongation of the N···H distance relative to the covalent bond distance, $\rho_{PT} = 0$. Values of ρ_{PT} calculated from the theoretical structures are also listed in Table 4.[55] Although the table contains structural results from MP2/aug-cc-pVDZ calculations only, we have also included the ρ_{PT} values obtained from similar calculations at the MP2/6-311++G(d,p) level to demonstrate the general level of consistency of conclusions regarding bonding for different basis sets. Note that this table is similar to that of Kurnig and Scheiner,[54] but the results have been obtained at a much higher level of computation.

It is apparent from the last column of Table 4 that the HF complexes are all hydrogen-bonded, with a slight, though steady, increase in a strongly negative value of ρ_{PT} between H_3N-HF and $(CH_3)_3N-HF$. The HCl and HBr complexes, on the other hand, undergo a distinct transition from hydrogen bonding to ion pair character with increasing methylation of the amine. Indeed, H_3N-HCl and H_3N-HBr are clearly hydrogen-bonded species, whereas $(CH_3)_3N-HCl$ and $(CH_3)_3N-HBr$ have more ionic than neutral character. The progression from HF to HCl to HBr for a particular amine is also accompanied by a clear increase in proton transfer. Note that, although the MP2/aug-cc-PVDZ and MP2/6-311++G(d,p) calculations concur in most respects, they differ in their prediction of the sign of ρ_{PT} for $(CH_3)_2HN-HCl$. The aug-cc-pVDZ basis set predicts predominantly ionic character for this species and the 6-311++G(d,p) basis predicts a more hydrogen-bonded complex. Indeed, generally speaking, the MP2/aug-cc-pVDZ calculations favor somewhat more proton transfer than do those done at the MP2/6-311++G(d,p) level. Nonetheless, both basis sets portray a consistent picture in which increasing methylation of the amine and/or increasing acidity of the HX moiety is accompanied by increased ion pair character. This result is in agreement with a preponderance of previous experimental and theoretical evidence.[1−10]

Energy Decomposition. The BLW decomposition of the binding energies is summarized in Table 5 and reveals further details of the interactions. The results are given for the MP2 optimized geometries and, though choice of geometry has some effect on the magnitude of individual energy terms, the important trends are preserved.[42] Consistent with the structural results, the energies also generally fall into two categories that follow the ionic and neutral interaction types. The hydrogen-bonded complexes have energy components that are significantly smaller in magnitude than the energy components of the ionized complexes. It is interesting to note, however, that although the energy components of the ion pairs are significantly greater in magnitude than those of the neutral pairs, the total interaction energies have about the same magnitude. In other words, even though the two types of complexes have dramatically different electronic structures, their net stabilities are similar. Thus, it is of interest to consider the individual energy components in more detail.

Referring to Table 5, the distortion energies show the trends expected from the structural considerations above. The total distortion energies for the HF complexes and other hydrogen-bonded complexes are low (∼1−5 kcal/mol), but those for the ion pairs range from ∼30 to 36 kcal/mol. In the HF complexes, the distortion energy of the HX monomer increases as the number of methyl groups on the amine is increased, reflecting the effect of acceptor basicity. The distortion energies of the amines are generally small but do increase slightly with an increasing amount of proton transfer.

The electrostatic and exchange energies are generally the largest in magnitude, not only for the aug-cc-pVDZ results given in Table 5 but also for all basis sets tested in this study. In the hydrogen-bonded complexes, these two terms are nearly equal to each other, differing only by a sign and resulting in a net electrostatic interaction energy exclusive of polarization ($\Delta E_{es} + \Delta E_{ex}$) of just a few kcal/mol. However, in the ionized complexes, the magnitude of the exchange term is approximately twice that of the electrostatic term. Thus, with the addition of each methyl group, there is an increased penetration of the proton into the electron cloud of the nitrogen lone pair electrons to create a stabilizing electrostatic interaction. Concomitantly, however, there is increased penetration of the hydrogen halide's electron density into the field occupied by the electrons localized on the amine. This creates a destabilizing exchange interaction. These processes occur simultaneously, but the exchange energy increases much faster, causing the $\Delta E_{(es+ex)}$ term to become more destabilizing as proton-transfer advances. Indeed, in the ion pairs, the electrostatic and exchange terms add up to a net repulsive energy in the range of 58−76 kcal/mol. For the hydrogen-bonded complexes, ΔE_{es+ex} is also repulsive, with the exception of H_3N-HF and $(CH_3)H_2N-HF$, for which these terms contribute −1.3 and −0.1 kcal/mol, respectively. Note, however, that this result is somewhat dependent on the geometry used for the BLW calculation: At the Hartree−Fock optimized geometry, the $\Delta E_{(es+ex)}$ term provides a net stabilization for all of the HF-amine complexes, with energies ranging from −3.9 kcal/mol in H_3N-HF to −1.9 kcal/mol in $(CH_3)_3N-HF$ using the aug-cc-pVDZ basis.

Most of the stabilization for both the neutral and ionic complexes arises from the polarization and charge-transfer terms. Moreover, Table 5 shows that the magnitudes of the polarization and charge-transfer energies increase as the degree of proton transfer increases. As the proton moves closer to the nitrogen (and the block-localized orbitals begin to occupy the same orbital space[56]), the energy associated with the relaxation of the monomer orbitals increase. Similarly, the charge-transfer energy term is high in the ion pairs due to the migration of a proton with significant orbital overlap with the nitrogen atom. The ion pairs exhibit nearly complete proton transfer that leads to dramatic changes in the electronic structure of each monomer. The large polarization and charge-transfer energies are a reflection of these changes. The calculations in Table 5 show that the polarization energies are significantly larger than the charge-transfer terms for the ion pairs, implying that the reorganization of charge density within each monomer is more pronounced in stabilizing the complex than the transfer of charge

between monomers. This result, however, is also basis set dependent. Indeed, using HF/6-311++G(d,p) energies from MP2/6-311++G(d,p) optimized geometries, the polarization and charge-transfer terms are nearly equal in energy. Thus, although both polarization and charge-transfer components are the origin of the stability of all the complexes studied, their relative contributions for the ionic species are system dependent, and the quantitative results depend on the specific basis sets used.

The electron correlation term, $\Delta\Delta E_{MP2}$, also contributes a significant amount to the total interaction energy, accounting for as much as 20−30% in the HF complexes. Interestingly, for the HF complexes, which are hydrogen-bonded, the magnitude of $\Delta\Delta E_{MP2}$ increases with increasing methylation, whereas the reverse is true for the HBr complexes, which are predominantly ionic for all but H_3N-HBr. In this light, the apparent irregularity seen for the series of HCl complexes (increasing initially down the series and then decreasing) is readily understood as a crossover which accompanies the change from hydrogen bonding to ion pair formation.

In summary, there is significant cancellation between the first-order Coulomb energy (ΔE_{es}) and the exchange term for all systems studied, leaving polarization as the dominant electrostatic contribution to the binding. However, the charge-transfer component is also significant, even in the most weakly bound members of the series. The appearance of conflicting energy terms is well-known for hydrogen-bonded systems,[50,53b,57,58] and it is interesting to see this feature persist into the proton-transferred regime. It is this cancellation of terms which gives rise to the relatively narrow range of binding energies in comparison with the wider variation in individual energy components across the series.

Electric Dipole Moment Decomposition and Atomic Charges. Table 6 displays the results of the BLW decomposition of the electric dipole moments investigated in this study. Recall that $\Delta\mu_{ind}^{BLW}$ is defined as the sum of five components (two distortion terms, two polarization terms, and a charge-transfer term), and $\Delta\mu_{ind}^{HF}$ is the total dipole moment of the complex minus the dipole moments of the free monomers. By comparing $\Delta\mu_{ind}^{BLW}$ to $\Delta\mu_{ind}^{HF}$, one sees that the BLW method yields reasonable agreement with the total Hartree−Fock induced dipole moment (typically within about 7%).

In all of the systems studied, the polarization terms contribute the most to the induced electric dipole moment, followed by smaller, but still significant, contributions from charge transfer. For the HF complexes, $\Delta\mu_{pol}$ of the amine is greater than $\Delta\mu_{pol}$ of the hydrogen halide. However, the reverse is true for complexes of HCl and HBr, consistent with their increased polarizability. Despite this reversal, however, it is remarkable to note that for all adducts studied, the polarization contribution to the induced dipole moment, $[\Delta\mu_{pol}(HX) + \Delta\mu_{pol}(amine)]$, is a nearly constant percentage of the total induced dipole moment, varying only between about 70% and 80% across the series. Only for $(CH_3)H_2N-HBr$, $(CH_3)_2HN-HBr$, and $(CH_3)_3N-HBr$ (i.e., the most ionic of the species) does this percentage climb into the 83−85% range.

For all complexes studied, most of the remainder of the induced dipole moment arises from charge transfer. This contribution is seen to be smaller for the neutral complexes, as expected, rising to as much as 0.93 D for $(CH_3)_3N-HBr$. The distortion terms, in general, are the least important contribution to $\Delta\mu_{ind}^{BLW}$ but do rise to as much as 0.44 D for the HCl component of $(CH_3)_3N-HCl$. In addition, it is seen in Table 6 that for all systems studied, the contributions due to distortion of the HX moiety exceeds that due to the amine. This is a reasonable result, inasmuch as any degree of proton transfer necessarily stretches the HX bond and, as noted above, a positive contribution from the HX distortion is to be expected. It is interesting to note, however, that the $\Delta\mu_{dist}$ components from the amines are actually slightly negative. Such an effect could arise from a slight flattening of the amine umbrella structure as the approach of a proton restricts the spatial extent of the lone pair.

In general, the induced electric dipole moment components due to distortion, polarization, and charge transfer all increase as methyl groups are added to the amine. This is consistent with trends in both proton affinity and polarizability, and parallels the trends observed in the energy decomposition analyses.

In Table 7, the charge transfer between monomers was estimated with Mulliken and natural population analyses (NPA).[52,53] Each isolated monomer has a charge of zero, but charge density is transferred between the monomers upon formation of the complex, resulting in a net partial charge on each monomer. Mulliken population analysis on the neutral dimers results in counterintuitive positive charges on the HX monomer, but it performs more reasonably on the complexes that exhibit a high degree of proton transfer. Natural population analysis appears to perform much better than the Mulliken population analysis for hydrogen-bonded complexes, and the two methods yield similar results for the ion pair complexes. The distinction between hydrogen bonding and ion pairing is clear, with the rather sharp divisions between the two types of complexes closely paralleling those revealed by bond lengths, energetics, and polarity. The NPA analysis for the amine-HF series, for example, shows a consistently small negative charge on the HF which increases with amine basicity, and the transition to ion pairing in the HCl and HBr series is accompanied by approximately a 10-fold increase in negative charge on the HX.

Conclusions

Benchmark values of the electric dipole moments of four amine−hydrogen halide complexes ($H_3{}^{15}N-H^{35}Cl$, $(CH_3)_3{}^{15}N-H^{35}Cl$, $H_3{}^{15}N-H^{79}Br$, and $(CH_3)_3{}^{15}N-H^{79}Br$) have been determined by rotational−Stark spectroscopy. The induced dipole moments are large and indicative of strong interactions. Theoretical decomposition of both the dipole moments and interaction energies using the Block Localized Wave function method has also been performed to elucidate the physical origins of the polarity and binding in these systems. The results are in accord with a large body of evidence indicating that HF forms hydrogen-bonded complexes with ammonia and all methylated forms of ammonia, but that there is a clear progression toward ion pair formation with the use of heavier hydrogen halides and more highly methylated amines. The induced dipole moments of both the hydrogen-bonded and ion-paired complexes arise predominantly from polarization, with the next most significant contribution due to charge transfer. The latter is smaller in the hydrogen-bonded systems than in the proton-transferred species but is still present. An interesting feature of the energy decomposition studies is that in both the neutral and ionic species, the binding energy arises from a rather complex interplay between terms. The electrostatic and exchange energies are of similar magnitudes but opposite signs, leading to significant cancellation of their contributions. Polarization and charge transfer dominate the binding in both the neutral and ionic complexes, though their relative contributions are both system and basis set dependent. Remarkably, the net stabilities of the hydrogen-bonded and ion-paired systems are quite comparable, with a range of binding energies much smaller than

the variations among individual energy components. Thus, in some sense, these systems belie their long standing reputation as "simple" systems in which to study hydrogen bonding and proton transfer.

Acknowledgment. The work was supported by the National Science Foundation, the University of Minnesota Supercomputer Institute, and the Army High-Performance Computing Research Center (AHPCRC) under the auspices of the Department of the Army, Army Research Laboratory DAAD 19-01-2-0014. M.C.O. was supported under the University of Minnesota Lando Undergraduate Research Program. J.K. was the recipient of an Undergraduate Research Fellowship from the Minnesota Supercomputer Institute, and the computations described in this paper were taken in part from his undergraduate honors thesis.

Supporting Information Available: Zero-field transition frequencies for $(CH_3)_3{}^{15}N-H^{79}Br$ and Stark-shifted transition frequencies for $H_3{}^{15}N-H^{35}Cl$, $(CH_3)_3{}^{15}N-H^{35}Cl$, $H_3{}^{15}N-H^{79}Br$, and $(CH_3)_3{}^{15}N-H^{79}Br$. This material is available free of charge via the Internet at http://pubs.acs.org.

References and Notes

(1) Goldfinger, P.; Verhaegen, G. *J. Chem. Phys*. **1969**, *50*, 1467.

(2) (a) Ault, B. S.; Pimentel, G. C. *J. Phys. Chem.* **1973**, *77*, 1649. (b) Ault, B. S.; Steinback, E.; Pimentel, G. C. *J. Phys. Chem*. **1975**, *79*, 615. (c) Barnes, A. J.; Orville-Thomas, W. J. *J. Mol. Struct.* **1978**, *45*, 75.

(3) See, for example (a) Barnes, A. J. *J. Mol. Struct.* **1980**, *60*, 343. (b) Johnson, G. L.; Andrews, L. *J. Am. Chem. Soc.* **1982**, *104*, 3043. (c) Schriver, L.; Schriver, A.; Perchard, J. P. *J. Am. Chem. Soc.* **1983**, *105*, 3843. (d) Barnes, A. J.; Beech, T. R.; Mielke, Z. *J. Chem. Soc., Faraday Trans. 2* **1984**, *80*, 455. (e) Barnes, A. J.; Kuzniarski, J. N. S.; Mielke, Z. *J. Chem. Soc., Faraday Trans. 2* **1984**, *80*, 465. (f) Barnes, A. J.; Wright, M. P. *J. Chem. Soc., Faraday Trans. 2* **1986**, *82*, 153. (g) Andrews, L.; Davis, S. R.; Johnson, G. L. *J. Phys. Chem.* **1986**, *90*, 4273.

(4) (a) Andrews, L.; Wang, X. *J. Phys. Chem. A* **2001**, *105*, 6420. (b) Andrews, L.; Wang, X.; Mielke, Z. *J. Am. Chem. Soc.* **2001**, *123*, 1499. (c) Andrews, L.; Wang, X.; Mielke, Z. *J. Phys. Chem. A* **2001**, *105*, 6054. (d) Andrews, L.; Wang, X. *J. Phys. Chem. A* **2001**, *105*, 7541. (e) Barnes, A. J.; Legon, A. C. *J. Mol. Struct.* **1998**, *448*, 101.

(5) Legon, A. C. *Chem. Soc. Rev.* **1993**, 153 and references therein.

(6) Hunt, S. W.; Higgins, K. J.; Craddock, M. B.; Brauer, C. S.; Leopold, K. R. *J. Am. Chem. Soc.* **2003**, *125*, 13850.

(7) Clementi, E. *J. Chem. Phys*. **1967**, *46*, 3851.

(8) See, for example: (a) Biczysko, M.; Latajka, Z. *J. Phys. Chem. A* **2002**, *106*, 3197. (b) Cherng, B.; Tao, F.-M. *J. Chem. Phys.* **2001**, *114*, 1720. (c) Alkorta, I.; Rozas, I.; Mó, O.; Yáñez, M.; Elguero, J.; *J. Phys. Chem. A* **2001**, *105*, 7481. (d) Tao, F.-M. *J. Chem. Phys.* **1999**, *110*, 11121. (e) Heidrich, D. *J. Mol. Struct. (THEOCHEM)* **1998**, *429*, 87. (f) Corongiu, G.; Estrin, D.; Murgia, G.; Paglieri, L.; Pisani, L.; Valli, G. S.; Watts, J. D.; Clementi, E. *Int. J. Quantum Chem.* **1996**, *59*, 119. (g) Heidrich, D.; van Eikema Hommes, J. R.; Schleyer, P. v. R. *J. Comput. Chem*. **1993**, *14*, 1149. (h) Latajka, Z.; Scheiner, S.; Ratajczak, H. *Chem. Phys. Lett*. **1987**, *135*, 367. (i) Brciz, A.; Karpfen, A.; Lischka, H.; Schuster, P. *Chem. Phys.* **1984**, *89*, 337. (j) Latajka, Z.; Scheiner, S. *J. Chem. Phys*. **1984**, *81*, 4014. (k) Latajka, Z.; Sakai, S.; Morokuma, K.; Ratajczak, H. *Chem. Phys. Lett*. **1984**, *110*, 464 and references therein.

(9) (a) Chaban, G. M.; Gerber, R. B.; Janda, K. C. *J. Phys. Chem. A* **2001**, *105*, 8323. (b) Snyder, J. A.; Cazar, R. A.; Jamka, A. J.; Tao, F.-M. *J. Phys. Chem. A* **1999**, *103*, 7719. (c) Biczysko, M.; Latajka, Z. *Chem. Phys. Lett.* **1999**, *313*, 366. (d) Li, R.-J.; Li, Z.-R.; Wu, D.; Hao, X.-Y.; Li, Y.; Wang, B.-Q.; Tao, F.-M.; Sun, C.-C. *Chem. Phys. Lett*. **2003**, *372*, 893.

(10) (a) Barnes, A. J.; Latajka, Z.; Biczysko, M. *J. Mol. Struct.* **2002**, *614*, 11. (b) Bevitt, J.; Chapman, K.; Crittenden, D.; Jordan, M. J. T.; Del Bene, J. E. *J. Phys. Chem. A* **2001**, *105*, 3371. (c) Jordan, M. J. T.; Del Bene, J. E. *J. Am. Chem. Soc*. **2000**, *122*, 2101. (d) Del Bene, J. E.; Jordan, M. J. T. *J. Chem. Phys.* **1998**, *108*, 3205. (e) Del Bene, J. E.; Jordan, M. J. T.; Gill, P. M. W.; Buckingham, A. D. *Mol. Phys.* **1997**, *92*, 429.

(11) (a) Mo, Y.; Peyerimhoff, S. D. *J. Chem. Phys*. **1998**, *109*, 1687. (b) Mo, Y.; Gao, J.; Peyerimhoff, S. D. *J. Chem. Phys*. **2000**, *112*, 5530.

(12) Mo, Y.; Zhang, Y.; Gao, J. *J. Am. Chem. Soc*. **1999**, *121*, 5737.

(13) (a) Mo, Y.; Gao, J. *J. Phys. Chem. A* **2001**, *105*, 6530. (b) Mo, Y.; Gao, J. *J. Phys. Chem. A*, in press.

(14) Balle, T. J.; Flygare, W. H. *Rev. Sci. Instrum*. **1981**, *52*, 33.

(15) (a) Phillips, J. A.; Canagaratna, M.; Goodfriend, H.; Grushow, A.; Almlöf, J.; Leopold, K. R. *J. Am. Chem. Soc*. **1995**, *117*, 12549. (b) Phillips, J. A. Ph.D. Thesis, University of Minnesota, 1996.

(16) Canagaratna, M.; Ott, M. E.; Leopold, K. R. *Chem. Phys. Lett*. **1997**, *281*, 63.

(17) Fiacco, D. L.; Mo, Y.; Hunt, S. W.; Ott, M. E.; Roberts, A.; Leopold, K. R. *J. Phys. Chem. A* **2001**, *105*, 484.

(18) Muenter, J. S. *J. Chem. Phys.* **1968**, *48*, 4544.

(19) Coudert, L. H.; Lovas, F. J.; Suenram, R. D.; Hougen, J. T. *J. Chem. Phys*. **1987**, *87*, 6290.

(20) (a) Legon, A. C.; Wallwork, A. L.; Rego, C. A. *J. Chem. Phys*. **1990**, *92*, 6397. (b) Gillies, C. W.; Gillies, J. Z.; Suenram, R. D.; Lovas, F. J.; Kraka, E.; Cremer, D. *J. Am. Chem. Soc.* **1991**, *113*, 2412.

(21) Canagaratna, M.; Phillips, J. A.; Goodfriend, H.; Leopold, K. R. *J. Am. Chem. Soc*. **1996**, *118*, 5290.

(22) Fiacco, D. L. Ph.D. Thesis, University of Minnesota, Minneapolis, MN, 2001.

(23) (a) *Organic Synthesis*, 2nd ed.; Wiley: New York, 1964; Collect. Vol. 1. (b) Clippard, P. H. Ph.D. Thesis, University of Michigan, 1969.

(24) Howard, N. W.; Legon, A. C. *J. Chem. Phys*. **1988**, *88*, 4694.

(25) Legon, A. C.; Rego, C. A. *J. Chem. Phys*. **1989**, *90*, 6867.

(26) Howard, N. W.; Legon, A. C. *J. Chem. Phys*. **1987**, *86*, 6722.

(27) Legon, A. C.; Wallwork, A. L.; Rego, C. A. *J. Chem. Phys*. **1990**, *92*, 6397.

(28) Gordy, W.; Cook, R. L. *Microwave Molecular Spectra*; John Wiley: New York, 1984.

(29) Kisiel, Z. PROSPE − Programs for Rotational Spectroscopy. http://info.ifpan.edu.pl/~kisiel/prospe.htm.

(30) Kisiel, Z.; Kosarzewski, J.; Pietrewicz, B. A.; Pszczó×b8kowski, L. *Chem. Phys. Lett.* **2000**, *325*, 523.

(31) Benz, H. P.; Bauder, A.; Gunthard, H. H. *J. Mol. Spectrosc.* **1966**, *21*, 156.

(32) Keenan, M. R.; Wozniak, D. B.; Flygare, W. H *J. Chem. Phys*. **1981**, *75*, 631.

(33) Read, W. G.; Flygare, W. H. *J. Chem. Phys.* **1982**, *76*, 2238.

(34) The difference likely results from the large nuclear quadrupole coupling constant in $^{15}NH_3\cdots H^{79}Br$ (361.091(12) MHz).

(35) Kaiser, E. W. *J. Chem. Phys*. **1970**, *53*, 1686.

(36) Van Dijk, F. A.; Dymanus, A. *Chem. Phys*. **1974**, *6*, 474.

(37) Marshall, M. D.; Muenter, J. S. *J. Mol. Spectrosc*. **1981**, *85*, 322. Note that although the value for $^{14}NH_3$ is used here, little error is expected to be incurred in calculating μ_{ind} for the $^{15}NH_3$ complexes.

(38) Lide, D. R.; Mann, D. E. *J. Chem. Phys.* **1958**, *28*, 572.

(39) Mo, Y.; Gao, J. BLW-ED version 1.0, University of Minnesota, Minneapolis, MN, 2004.

(40) Frisch, M. J.; Trucks, G. W.; Schlegel, H. B.; Scuseria, G. E.; Robb, M. A.; Cheeseman, J. R.; Montgomery, J. A., Jr.; Vreven, T.; Kudin, K. N.; Burant, J. C.; Millam, J. M.; Ilyengar, S. S.; Tomasi, J.; Barone, V.; Mennucci, B.; Cossi, M.; Scalmani, G.; Rega, N.; Petersson, G. A.; Nakatsuji, H.; Hada, M.; Ehara, M.; Toyota, K.; Fukuda, R.; Hasegawa, J.; Ishida, M.; Nakajima, T.; Honda, T.; Kitao, O.; Nakai, H.; Klene, M.; Li, X.; Knox, J. E.; Hratchian, H. P.; Cross, J. B.; Bakken, V.; Adamo, C.; Jaramillo, J.; Gomperts, R.; Stratmann, R. E.; Yazyev, O.; Austin, A. J.; Cammi, R..; Pomelli, C.; Ochterski, J. W.; Ayala, P. Y.; Morokuma, K.; Voth, G. A.; Salvador, P.; Dannenberg, J. J.; Zakrzewski, V. G.; Dapprich, S.; Daniels, A. D.; Strain, M. C.; Farkas, O.; Malick, D. K.; Rabuck, A. D.; Raghavachari, K.; Foresman, J. B.; Ortiz, J. V.; Cui, Q.; Baboul, A. G.; Clifford, S.; Cioslowski, J.; Stefanov, B. B.; Liu, G.; Liashendo, A.; Piskorz, P.; Komaromi, I.; Martin, R. L.; Fox, D. J.; Keith, T.; Al-Laham, M. A.; Peng, C. Y.; Nanayakkara, A.; Challacombe, M.; Gill, P. M. W.; Johnson, B.; Chen, W.; Wong, M. W.; Gonzalez, C.; Pople, J. A. *Gaussian 03*, revision C.01; Gaussian, Inc.: Wallingford, CT, 2004.

(41) Boys, S. F.; Bernardi, F. *Mol. Phys*. **1970**, *19*, 553.

(42) Kilian, J. Honors Thesis, University of Minnesota, Minneapolis, MN, 2005.

(43) Pawlowski, F.; Jørgensen, P.; Olsen, J.; Hegelund, F.; Helgaker, T.; Gauss, J.; Bak, K. L.; Stanton, J. F. *J. Chem. Phys.* **2002**, *116*, 6482.

(44) De Lucia, F. C.; Helminger, P.; Gordy, W. *Phys Rev. A* **1971**, *3*, 1849.

(45) Helminger, P.; De Lucia, F. C.; Gordy, W. *J. Mol. Spectrosc*. **1971**, *39*, 94.

(46) Muenter, J. S. *J. Chem. Phys*. **1972**, *56*, 5409.

(47) Rosmus, P.; Botschwina, P.; Werner, H.-J.; Vaida, V.; Engelking, P. C.; McCarthy, M. I. *J. Chem. Phys*. **1987**, *86*, 6677.

(48) Jeziorski, B.; Moszynski, R.; Szalewicz, K. *Chem. Rev.* **1994**, *94*, 1887.

(49) van der Vaart, A.; Merz, K. M., Jr. *J. Phys. Chem. A* **1999**, *103*, 3321.

(50) Kitaura, K.; Morukuma, K. *Int. J. Quantum Chem*. **1976**, *10*, 325.

(51) Glendening, E. D.; Streitwieser, A. *J. Chem. Phys*. **1994**, *100*, 2900.

(52) Glendening, E. D.; Reed, A. E.; Carpenter, J. E.; Weinhold, F. NBO Version 3.1.

(53) (a) Foster, J. P.; Weinhold, F. *J. Am. Chem. Soc.* **1980**, *102*, 7211. (b) Reed, A. E.; Weinhold, F. *J. Chem. Phys.* **1983**, *78*, 4066. (c) Reed, A. E.; Weinstock, R. B.; Weinhold, F. *J. Chem. Phys.* **1985**, *83*, 735. (d) Reed, A. E.; Weinhold, F.; Curtiss, L. A.; Pochatko, D. J. *J. Chem. Phys.* **1986**, *84*, 5687. (e) Reed, A. E.; Curtiss, L. A.; Weinhold, F. *Chem. Rev.* **1988**, *88*, 899.

(54) Kurnig, I. J.; Scheiner, S. *Int. J. Quantum Chem., Quantum Biol. Symp.* **1987**, *14*, 47.

(55) The value of r^o(N−H) for these calculations has been taken as that in free NH_3.

(56) Here, the space refers to a set of basis functions, not a physical three-dimensional definition. "The same space" means that the BLW orbitals are still expanded with the basis functions in one monomer but the coefficients will vary (i.e., electron density will reshape) in response to the approach of the other monomer.

(57) Huang, D.-M.; Wang, Y.-B.; Visco, L. M.; Tao, F.-M. *Chem. Phys. Lett.* **2005**, *407*, 222.

(58) Jeffrey, G. A. *An Introduction to Hydrogen Bonding*, Oxford University Press: New York, 1997; see also references therein.